Zonal intermediate currents in the equatorial Atlantic Ocean

Michel Ollitrault,[1] Matthias Lankhorst,[2] David Fratantoni,[3] Philip Richardson,[3] and Walter Zenk[2]

Received 1 December 2005; revised 26 January 2006; accepted 30 January 2006; published 7 March 2006.

[1] Acoustic float data collected near 800 m depth, are used to map zonal mean currents within the Antarctic Intermediate Water (AAIW) tongue in the equatorial Atlantic. Alternating zonal jets of 2° latitudinal width are revealed between 6°S and 6°N. Displacements from profiling floats drifting near 1000 m depth, also reveal similar zonal jets at the base of the AAIW layer. The strongest jets (15 cm s^{-1} peak) are found at 4°S, 2°S, 0°, 2°N and 4°N. They are coherent longitudinally over order of 3000 km and, poleward of 1°S and 1°N, generally coherent vertically between 800 m and 1000 m. Large seasonal fluctuations exist at both levels: within 1° of equator, AAIW at 800 m flows westward (8 cm s^{-1} mean) in boreal summer and fall but eastward (3 cm s^{-1} mean) in winter, whereas the flow at 1000 m is eastward in late fall and winter. **Citation:** Ollitrault, M., M. Lankhorst, D. Fratantoni, P. Richardson, and W. Zenk (2006), Zonal intermediate currents in the equatorial Atlantic Ocean, *Geophys. Res. Lett.*, *33*, L05605, doi:10.1029/2005GL025368.

1. Introduction

[2] In the equatorial Atlantic, Antarctic Intermediate Water (AAIW), whose core is traced by a minimum in salinity around 750 m depth, is found at depths between 500 m and 1000 m (Figure 1). Meridional hydrographic sections at 30°W [*Mémery et al.*, 2000], 25°W [*Tsuchiya et al.*, 1992, 1994], 8°W and 5°E [*Mercier et al.*, 2003] all show at the core of minimum salinity, a slight oxygen maximum near 2°S which decreases eastward and almost disappears in the easternmost section. This indicates an eastward flow from the western boundary where an intermediate western boundary current named the North Brazil Undercurrent (NBUC) flows equatorward from the subtropical southern latitudes, bringing relatively high oxygenated AAIW waters [*Suga and Talley*, 1995; *Boebel et al.*, 1999].

[3] During the World Ocean Circulation Experiment (WOCE) and since then, many top to bottom Acoustic Doppler Current Profiler (ADCP) meridional sections were realised within 5° of the equator. These snapshots reveal vertically alternating eastward and westward stacked jets at the Equator, the eastward Equatorial Undercurrent (EUC) being the shallowest and strongest [*Gouriou et al.*, 2001]. They also disclose latitudinally alternating zonal jets, north and south of the equator. At the AAIW level, besides the eastward flow already diagnosed with oxygen around 2°S, named [*Stramma and England*, 1999] the Southern Intermediate Counter Current (SICC), there are at least two other fast jets: a generally westward jet centered at the Equator and an eastward jet around 2°N, named respectively the Equatorial Intermediate Current (EIC) and the Northern Intermediate Counter Current (NICC) [*Bourlès et al.*, 2003; *Schott et al.*, 2003, 2005]. Such a complicated "instantaneous" structure of equatorial flows is not attainable with classical hydrography since geostrophy fails near the equator.

[4] Subsurface floats offer another way to measure equatorial (absolute) currents, in particular their time evolution, although generally restricted to one or a few levels [e.g., *Schmid et al.*, 2003]. In this paper, we use a large float database collected over the last 10 years to estimate the mean zonal circulation around 800 m and 1000 m depths, between 12°S and 12°N. We also investigate the seasonal variability of the zonally averaged zonal currents.

2. Float Data

[5] Two different types of floats are used in this study: acoustically tracked floats at 800 m, profiling floats (without acoustic tracking) at 1000 m.

[6] Acoustic floats are of the RAFOS type: they receive acoustic signals sent by moored sound sources, and reemit the times of arrival of the signals received, via the ARGOS satellite system, after surfacing [*Rossby et al.*, 1986]. Data processing later provides daily positions at depth. Original RAFOS floats ascend only once at the end of their mission (order 1 year) at depth, while MARVOR floats [*Ollitrault et al.*, 1994] cycle periodically (e.g., every 3 months) between their mission depth and the surface.

[7] Profiling floats are of the ALACE type: they drift at depth, like acoustic floats, but return frequently to the surface where they are located by satellite [*Davis et al.*, 1992]. With 11-day cycles, they generally provide 10-day displacements at depth, estimated from surface fixes. They also profile temperature and salinity during the ascents. Besides the original profiling ALACE (or P-ALACE), several versions (APEX, PROVOR, SOLO, ...) are now in use within the ARGO project, whose aim is to cover the whole ocean with at least 1 float in every 3° × 3° square.

[8] Over 110 years of MARVOR (90% of total) and RAFOS float data, collected between March 1994 and October 2003, within the 750–850 dbar pressure range and between 12°S and 12°N, are used to map the zonal mean currents near AAIW core. Within the 950–1050 dbar pressure range, the zonal mean circulation is estimated from 165 years of ARGO (90% of total) and P-ALACE float data, collected between January 1997 and April 2005, over the same region.

[1] Institut français de Recherche pour l'Exploitation de la mer, Plouzané, France.
[2] Institut für Meereswissenschaften-GEOMAR, Kiel, Germany.
[3] Woods Hole Oceanographic Institute, Woods Hole, Massachusetts, USA.

0094-8276/06/2005GL025368$05.00

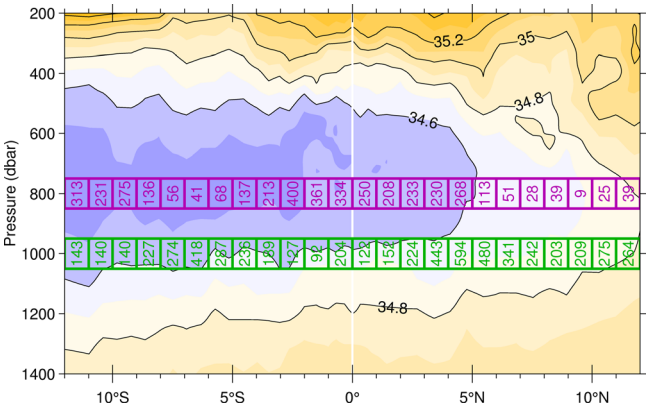

Figure 1. Salinity section along approximately 25°W, from *Tsuchiya et al.* [1992, 1994]. Number of 10-day float displacements within each one degree of latitude zonal band (America to Africa), between 750 and 850 dbar (magenta) and between 950 and 1050 dbar (green).

[9] Errors on satellite fixes, and displacements induced as profiling floats ascent or descent may contribute an error of 3 mm s^{-1} on the estimated 10-day mean currents at depth [*Davis and Zenk*, 2001]. However, order of 2 hours delay in surface positioning can add a 1 cm s^{-1} error, whence a total (measurement) error of order 1 cm s^{-1}.

[10] Accuracy of acoustic float daily positions is of the order of a few km. However 10-day mean currents, used in this study, are obtained from the corresponding displacements at depth, whose relative end positions are generally more accurate (possibly order of 1 km), implying a few mm s^{-1} error only.

3. Mean Zonal Currents Near 800 m and 1000 m Depths

[11] Assuming time stationarity on a multi-year time scale, zonal mean currents are shown on Figures 2a and 2b for the upper and lower ranges respectively. A series of alternating westward (blue) and eastward (red) currents roughly every 2° of latitude emerges clearly between 12°S and at least 8°N, although lack of acoustic float data almost precludes the observation south of 5°S and north of 6°N, at the 800 m level. This zonal banded structure stretches from the western boundary to the Greenwich meridian. At the 1000 m level, the signal is generally stronger west of the Mid-Atlantic Ridge (MAR). South of equator the bands are quasi zonal, but are slightly slanted in the northern hemisphere, possibly because of the topographic constraint of the continental masses (America and Africa) and influence of the MAR running WNW, north of equator.

[12] At the upper level, the westward flowing EIC, centered on the equator, the SICC and NICC centered 2°S and 2°N respectively, both flowing eastward and the two westward mean currents centered 4°S and 4°N, called South and North Equatorial Intermediate Currents (SEIC and NEIC [*Firing et al.*, 1998]) are strong features of the intermediate equatorial circulation with peak mean velocities exceeding 10 cm s^{-1}. These five zonal mean jets are coherent longitudinally over more than 3000 km, at least for this multiyear average. South of 5°S, on the western side, there are indications that a zonal banded structure is present.

[13] At the lower level, the mean zonal circulation is not so clear cut between 1°S and 2°N, possibly because of lack of data. Within 1° of equator, the flow is eastward over the MAR where it shallows to less than 3000 m, between 30°W and 15°W. West and East of these longitudes, the flow is westward, similar to the 800 m level. At 35°W a mean of 13 ADCP sections, taken between 1990 and 2002, also shows a westward flow at 1000 m [*Schott et al.*, 2003], while a few sections taken between 30°W and 15°W tend to support an eastward flow at 1000 m [*Schmid et al.*, 2005]. Since the vertical scale of the stacked jets at the equator is of the order of 500 m [*Gouriou et al.*, 2001] we may not expect the same signal at 800 m and 1000 m. A west to east (from 1000 m to 1200 m depth) deepening of the EIC [*Schmid et al.*, 2005] may also preclude the exact mapping of the jet, with floats drifting at constant depth. However, the coincidence of the reversal of the 1000 m flow with the shallow MAR, at the equator, could suggest a topographic influence. Near 2°S, the SICC is well defined, flowing eastward from the western boundary to at least 12°W where it reaches the MAR, with peak mean zonal velocities of 15 cm s^{-1} found in the west. Lack of data above the MAR crest however, prevents us from concluding whether there is a MAR influence on SICC.

[14] That the SICC, at both levels, can be traced back to the lower part of NBUC, is verified with the vector mean float circulation (not given here). Actually, examination of individual trajectories and displacements show confused and slower motions near 2°S–3°S and 40°W with only a small fraction of the floats finding their way northward to the equator, along the western boundary.

[15] The deep NICC, although generally flowing eastward, like at upper level, is not well defined too because of

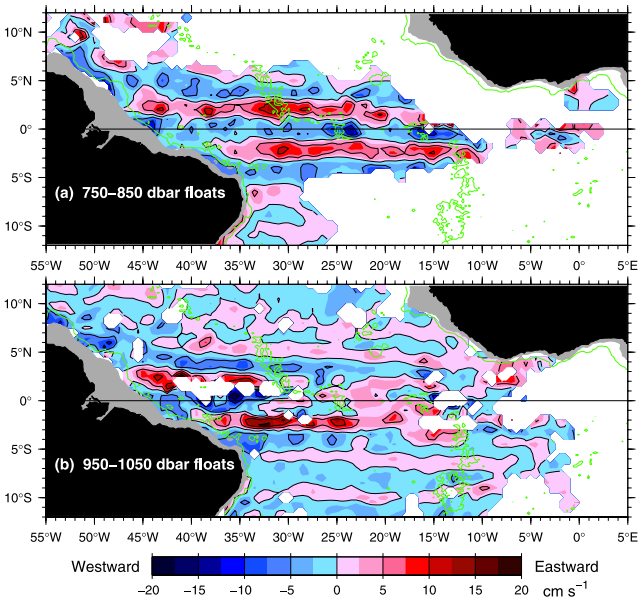

Figure 2. Mean zonal currents obtained as weighted averages (Gaussian with a 50 km standard deviation) of 10-day zonal float velocities: (a) for the upper range near the core of AAIW tongue, (b) for the lower range at the base of AAIW tongue. One month of data, at least, for each grid point contoured. The 3000 m isobath is outlined in green.

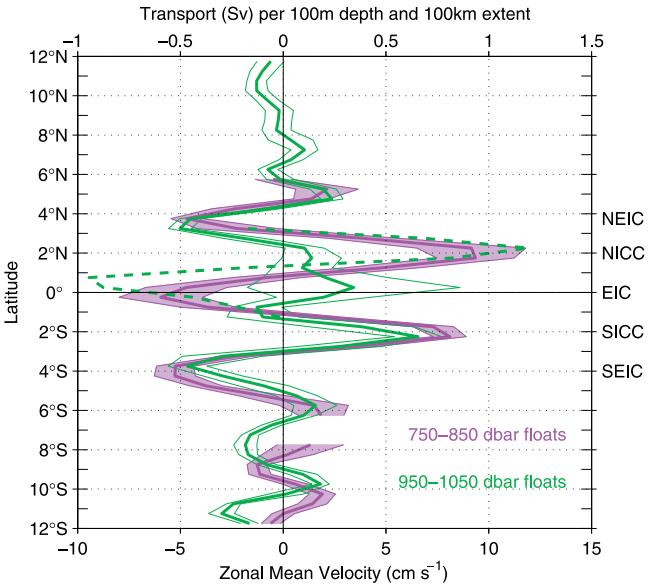

Figure 3. Mean zonal currents averaged over 33°W to 20°W. Error on the mean is obtained from the 10-day zonal velocity sample variance (mesoscale variability) and a number of degrees of freedom (at least 7) estimated as half the 10-day "sample" number. Dashed green curve shows, for the lower range, between 1°S and 3°N, the mean zonal currents averaged west of the Mid-Atlantic Ridge.

gappy data. Poleward, the mean zonal circulation is better defined. The deep SEIC and NEIC are coherent longitudinally over 4000 km and seemingly quasi-coherent vertically with the upper SEIC and NEIC. There is a weak but clear eastward flow (2 cm s^{-1} peak mean) near 6°S, a westward flow near 7–8°S (4 cm s^{-1} peak mean) and an eastward flow at 9–10°S (3 cm s^{-1} peak mean). North of NEIC, there is also an eastward flow near 6°N (but around 4°N at 15°W) of order 3 cm s^{-1} peak mean. Further north, the quasi-zonal (in fact slightly slanted) alternating structure is not as visible as its southern counterpart.

[16] Figure 3 shows the mean zonal currents, zonally averaged between 33°W and 20°W, with the corresponding errors obtained from mesoscale variability only, since measurement errors on the means are negligible with large sample numbers. This modest longitudinal breadth was chosen to avoid the bias caused by the slanting bands. The mean zonal structure in the upper range is quasi-symmetrical relatively to the Equator, with a slight shortening of jet widths poleward: for example, the northern counterpart of the eastward flow at 6°S is found rather near 5°N. The lower range zonally averaged flow structure is almost indistinguishable, within errors, from the upper one, except between 1°S and 2°N and south of 7°S. The 63% confidence intervals (order of ±1 cm s^{-1}) are much smaller than the resolved mean signals everywhere, except near 1000 m, between 1°S and 2°N, revealing there both an uneven distribution of data over time and space and possibly a greater intrinsic variability. Thus, except for the EIC and NICC, all these quasi-zonal jets are coherent vertically (between 800m and 1000m) between 6°S and 6°N. Southward, a phase shift is apparent between the two levels. Note also that, if we average data for the lower range, but only west of the MAR crest, we recover a strong westward EIC and a strong eastward NICC, similar to the upper range signals.

[17] Assuming a 500 m thick AAIW layer, and using the upper range zonal mean currents, we obtain the following transports (in 10^6 m^3 s^{-1} or *Sv*): −5.2 ± 0.6 *Sv* (SEIC), 6.0 ± 0.6 *Sv* (SICC), −4.3 ± 0.9 *Sv* (EIC), 6.4 ± 1.1 *Sv* (NICC) and −2.8 ± 0.6 *Sv* (NEIC), comparable with *Schott et al.* [2005] estimates at 35°W (ADCP section).

4. Seasonal Fluctuations of the AAIW Zonal Flows

[18] Figure 4 shows the zonal currents zonally averaged between 33°W and 20°W, for the upper range (750–850 dbar) and for each month (Hovmöller plot). This allows to concentrate on seasonal fluctuations only. Interannual fluctuations also exist [*Schmid et al.*, 2005], but are outside the scope of this study.

[19] The alternating westward and eastward flows, every 2° of latitude, are still present, although south of 5°S, the float data covers only the region west of 26°W. Strong seasonal signals are visible between 5°S and 5°N. On the equator, the EIC flows generally westward and reaches −10 cm s^{-1} during boreal fall, but reverses eastward (+3 cm s^{-1}) during boreal winter (January and February). Meanwhile, SICC and NICC, never change direction over the year but are found nearer to equator (1°30′S and 1°30′N) in late winter and early spring. Their strength and latitudinal extent vary in phase (reaching 10 cm s^{-1} in early summer and being thinner in autumn). Similarly, SEIC and NEIC are both stronger in early spring. In the lower range (950–1050 dbar), there are also strong seasonal variations, but the data are slightly more gappy near the equator.

[20] Figure 5 shows the harmonic analysis of the monthly zonal currents, for both upper range and lower range. *Schott et al.* [2003] explain 90 % of the EIC fluctuations at 700–900 m depth and 35°W (ADCP data) with an annual plus a semi-annual harmonics, with a strong westward flow in fall, similar to our results. They find however an eastward EIC

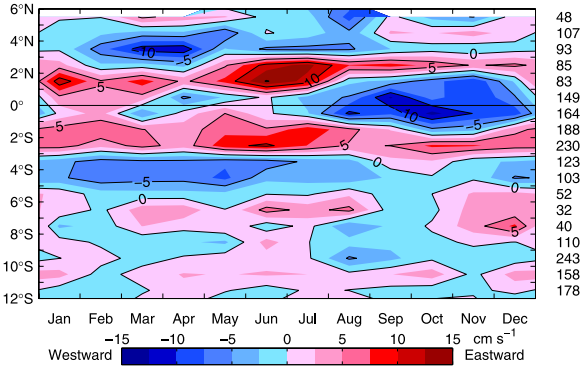

Figure 4. Seasonal variations of the mean zonal currents, in the upper range (750–850 dbar), after averaging within each month (all years combined) and between 33° W and 20° W. Numbers of 10-day displacements for each one degree of latitude, on the right. 30 days of data, at least, for each grid point contoured, except for a few ones around 7°S.

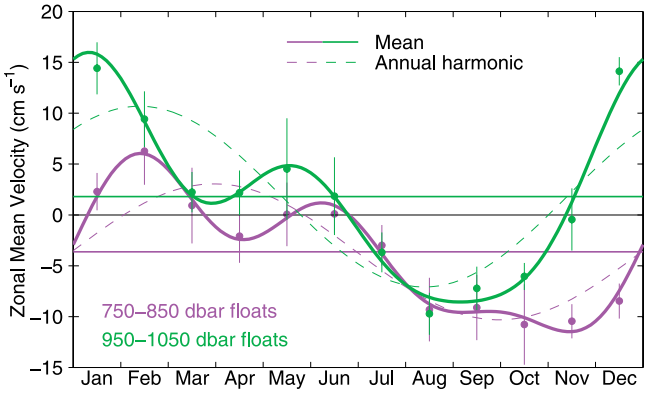

Figure 5. Harmonic analysis of the monthly zonal mean current within one degree of equator. Dots and vertical bars indicate monthly mean values and their errors. Thick curves give the synthesis using the mean, annual, semi-annual and fourth-monthly harmonics.

around June–July, whereas we find such a reverse flow in February and possibly in June. Note the phase delay between the upper and lower levels, which may be due to Rossby wave upward phase propagation, while energy propagates downward [*Thierry et al.*, 2004]. Using data only west of the MAR crest, does give different results at 1000 dbar, but brings no significant changes at 800 dbar. On an other hand, plots (not shown) of the 800 dbar and 1000 dbar zonal currents (as on Figure 2), for each of the four seasons, reveal that the EIC (and the two ICC) are longitudinally coherent over 2000 to 3000 km. However, lack of data at 1000 dbar, prevents from concluding whether the deep reversing mean flow seen on the equator (Figure 2b) is caused by an uneven distribution of the profiling floats, a strong seasonal variability or a topographic influence, or a combination of these.

5. Concluding Remarks

[21] Alternating zonal jets centred approximately every 2° in latitude, and symmetrical relatively to the Equator are clearly revealed by a multi-year averaging of float data at intermediate depths (800 m and 1000 m) between 6°S and 6°N. The EIC, SICC, NICC, SEIC and NEIC, are robust features of the Atlantic equatorial circulation (even, if their strength and width may vary during the year). The EIC at 1000 m is not satisfactorily resolved, however this will be remedied as more ARGO data are available.

[22] Such equatorial zonal jets at AAIW level have also been diagnosed recently by high resolution primitive equation numerical models. *Tréguier et al.* [2003] obtain alternating zonal jets, between 12°S and 5°N, agreeing latitudinally with our observations but with velocities (averaged over 10 years) much weaker (order of 1 cm s^{-1}). In the equatorial Pacific, *Nakano and Hasumi* [2005] also find alternating zonal jets (after a 5-year averaging) with similar latitudinal widths and weak zonal velocities.

[23] **Acknowledgments.** MARVOR floats were deployed during the SAMBA experiment, which was the main French participation to the WOCE subsurface float program. Costs were supported by IFREMER. RAFOS floats from IFM-GEOMAR were also deployed as the German participation to the WOCE subsurface float program. Costs were supported through contracts DFG Ze 145/7-1 and BMFT Fkz 03F0157A. Besides P-ALACE data from WHOI, all profiling float data, near 1000 m depth, were collected and made freely available by the international ARGO Project and the national programs that contribute to it.

References

Boebel, O., R. Davis, M. Ollitrault, R. Peterson, P. Richardson, C. Schmid, and W. Zenk (1999), The intermediate depth circulation of the western South Atlantic, *Geophys. Res. Lett.*, *26*(21), 3329–3332.

Bourlès, B., et al. (2003), The deep currents in the eastern equatorial Atlantic Ocean, *Geophys. Res. Lett.*, *30*(5), 8002, doi:10.1029/2002GL015095.

Davis, R., and W. Zenk (2001), Subsurface Lagrangian observations during WOCE, in *Ocean Circulation and Climate, Int. Geophys. Ser.*, vol. 77, pp. 123–139, Elsevier, New York.

Davis, R., D. Webb, L. Regier, and J. Dufour (1992), The autonomous Lagrangian circulation explorer (ALACE), *J. Atmos. Oceanic Technol.*, *9*, 264–285.

Firing, E., S. Wijffels, and P. Hacker (1998), Equatorial subthermocline currents across the Pacific, *J. Geophys. Res.*, *103*(C10), 21,413–21,423.

Gouriou, Y., et al. (2001), Deep circulation in the equatorial Atlantic Ocean, *Geophys. Res. Lett.*, *28*(5), 819–822.

Mémery, L., M. Arhan, X. Alvarez-Salgado, M.-J. Messias, H. Mercier, C. Castro, and A. Rios (2000), The water masses along the western boundary of the south and equatorial Atlantic, *Prog. Oceanogr.*, *47*, 69–98.

Mercier, H., M. Arhan, and R. Lutjeharms (2003), Upper-layer circulation in the eastern equatorial and south Atlantic ocean in January-March 1995, *Deep Sea Res., Part I*, *50*, 863–887.

Nakano, H., and H. Hasumi (2005), A series of zonal jets embedded in the broad zonal flows in the Pacific obtained in eddy-permitting ocean general circulation models, *J. Phys. Oceanogr.*, *35*, 474–488.

Ollitrault, M., G. Loaec, and C. Dumortier (1994), MARVOR: A multi-cycle RAFOS float, *Sea Technol.*, *35*(2), 39–44.

Rossby, T., D. Dorson, and J. Fontaine (1986), The RAFOS system, *J. Atmos. Oceanic Technol.*, *3*, 672–679.

Schmid, C., Z. Garraffo, E. Johns, and S. Garzoli (2003), Pathways and variability at intermediate depths in the tropical Atlantic, in *Interhemispheric Water Exchange in the Atlantic Ocean, Oceanogr. Ser.*, vol. 68, pp. 233–268, Elsevier, New York.

Schmid, C., B. Bourlès, and Y. Gouriou (2005), Impact of the equatorial deep jets on estimates of zonal transports in the Atlantic, *Deep Sea Res., Part II*, *52*, 409–428.

Schott, F., M. Dengler, P. Brandt, K. Affler, J. Fischer, B. Bourlès, Y. Gouriou, R. Molinari, and M. Rhein (2003), The zonal currents and transports at 35°W in the tropical Atlantic, *Geophys. Res. Lett.*, *30*(7), 1349, doi:10.1029/2002GL016849.

Schott, F., M. Dengler, R. Zantopp, L. Stramma, J. Fischer, and P. Brandt (2005), The shallow and deep western boundary circulation of the south Atlantic at 5–11°S, *J. Phys. Oceanogr.*, *35*, 2031–2053.

Stramma, L., and M. England (1999), On the water masses and mean circulation of the south Atlantic Ocean, *J. Geophys. Res.*, *104*(C9), 20,863–20,883.

Suga, T., and L. Talley (1995), Antarctic Intermediate Water circulation in the tropical and subtropical south Atlantic, *J. Geophys. Res.*, *100*(C7), 13,441–13,453.

Thierry, V., A.-M. Tréguier, and H. Mercier (2004), Numerical study of the annual and semi-annual fluctuations in the deep equatorial Atlantic Ocean, *Ocean Modell.*, *6*, 1–30.

Tréguier, A.-M., N. Hogg, M. Maltrud, K. Speer, and V. Thierry (2003), The origin of deep zonal flows in the Brazil basin, *J. Phys. Oceanogr.*, *33*, 580–599.

Tsuchiya, M., L. Talley, and M. McCartney (1992), An eastern Atlantic section from Iceland southward across the equator, *Deep Sea Res.*, *39*, 1885–1917.

Tsuchiya, M., L. Talley, and M. McCartney (1994), Water-mass distribution in the western South Atlantic: A section from South Georgia Island (54S) northward across the equator, *J. Mar. Res.*, *52*, 55–81.

D. Fratantoni and P. Richardson, Woods Hole Oceanographic Institution, M.S. 21, Woods Hole, MA 02543, USA. (dfratantoni@whoi.edu; prichardson@whoi.edu)

M. Lankhorst and W. Zenk, Leibniz-Institut für Meereswissenschaften, Düsternbrooker Weg 20, D-24105 Kiel, Germany. (mlankhorst@ifm-geomar.de; wzenk@ifm-geomar.de)

M. Ollitrault, Institut français de Recherche pour l'Exploitation de la mer, Centre de Brest, B.P. 70, F-29280 Plouzané, France. (mollitra@ifremer.fr)